HUNTINGTON MEDICAL RESEARCH INSTITUTES
NEUROLOGICAL RESEARCH LABORATORY
734 Fairmount Avenue
Pasadena, California 91105

Contract No. NO1-NS-5-2324

QUARTERLY PROGRESS REPORT
January 31 - March 31, 1995

Report No. 1

"SAFE AND EFFECTIVE STIMULATION OF NEURAL TISSUE"

William F. Agnew, Ph.D.
Douglas B. McCreery, Ph.D.
Ted G.H. Yuen, Ph.D.
Randy R. Carter, Ph.D.
Leo A. Bullara, B.A.

This QPR is being sent to you before it has been reviewed by the staff of the Neural Prosthesis Program

ABSTRACT

Since the January 1, 1994 QPR which reported results with active intracortical electrode arrays, a total of 19 passive arrays were implanted in the cerebral cortex of 11 cats (Table 1). Of these, one cat received bilateral implants of 4 individual iridium electrodes while another cat was implanted unilaterally with a 7-electrode array. This array was salvaged from IC-100 and reused in IC-105. Each of two other cats received a unilateral implant of 9 iridium electrodes. Nine array of 4 x 4 photolithographic (University of Michigan) electrodes were implanted either unilaterally or bilaterally in 6 cats. For technical reasons three of these implants in one cat were excluded from the study. Finally, one cat received 3 implants: one 2 x 2 and a 7-electrode array (iridium) and a single photolithographic (University of Michigan) probe. Following implant durations of 2 to 69 days, the animals were sacrificed and the tissues prepared for paraffin sections and examination by light microscopy. A wide spectrum of results was found in the probe areas and included hemorrhage, gliosis, hyperplasia and hypertrophy of blood vessels.

INTRODUCTION

This report examines the biocompatibility and tissue response following implantation of iridium and silicon microprobes into brain cortex, taking into account the insertion speed, variations in methods of implantation (piston held by an electrode carrier drive vs. manual) and the nature of the biomaterials (e.g., epoxylite, iridium and silicon). In two of the 11 animals, a preliminary study involved the use of non-beveled, rounded-tip probes as opposed to probes having the usual 20° or 30° bevel angle.

METHODS

Electrode fabrication. Fifty μm diameter iridium shafts were electrochemically etched in a saturated solution of NaCl using a carbon rod as a counter electrode. A 30 volt AC potential was applied between the carbon rod and iridium shafts attached to a multiple electrode holder. The desired 10° angle cone was fashioned by submerging and withdrawing the shafts from the solution over a 3 minute period, giving a reasonably smooth conical surface. The electrode tips were beveled to an angle of 20° to form ellipsoidal facets.

TABLE 1
PASSIVE IMPLANTS

IC #	# OF PROBES	MATERIAL	METH. OF INSERTION	IMPLANT DURATION (DAYS)	SURGERY (OBSERVATIONS)	AUTOPSY (OBSERVATIONS)	HISTOLOGY			
							NEU-RONS	HEM. CAV.	GLIO-SIS	VASC. PROLIF.
87-L	9	IR	M	21	----------	----------	N	+++	+++	0
91-L	9	IR	M	24	----------	----------	N	0	+	0
93-L	16	Si	S	58	Array shifted during suturing of dura.	5 probes fractured. Left in brain.	N	0	++	0
94-L	16	Si	S	69	2 attempts to penetrate pial dimpling.	2 probes left in cortex.	N	0	0	+
97-L	16	Si		41	Stereotaxic penetr. unsuccessful - impl. manually.	7 shafts left in cortex.		0	+++	0
98-L	16	Si	S	24	Stereotaxic penetr. unsuccessful - impl. manually.	Hemorr. over array site. Some probes left in cortex.		0	0	0
99-L	16	Si	S	29	Stereotaxic penetr. unsuccessful - impl. manually.	3 probes left in cortex.			+++	0
99-R	16	Si	S	29	Stereotaxic penetr. unsuccessful - impl. manually.	6 probes left in cortex.		+++	+++	0
100-R	7	IR	S	42	Heavier stereotaxic device. Good penetr.	----------		0	+++	0
104-L	4	IR	M	2	----------	----------		+++	0	0
104-R	4	IR	M	2	----------	----------		++	0	0
105-L	4	IR	M	34	----------	Array lifted with dura.		0	++	++
105-R	7	IR	M	34	Re-used array from IC-100	Array lifted with dura		+++	0	0
105-R	1	Si	M	34	----------	Probe not found.		0	0	0

CODE:
M = Manual insertion
S = Stereotaxic insertion (piston & sleeve)
H = Hemorrhage
CAV.= Cavitation
+ = Slight ++ = Moderate
+++ = Marked

PROBE LENGTHS:
IRIDIUM IC-105 = Approx. 2.8 mm. No bevel. Epoxylite-coated.
All others = Approx. 1.6 mm. Epoxylite-coated.
PHOTOLITHOGRAPHIC Approx. 1.3 mm

PROBE DIAMETERS
IRIDIUM: IC-87 = 73 µm; All others = approx. 51 µm
PHOTOLITHOGRAPHIC = 15 X 30 µm (cross section).

After formation of the cone, the electrode tips were abraded by "peening" with 27 μm Al_2O_3 particles to form a uniformly rough surface to improve bonding of the Epoxylite insulation. The residual Al_2O_3 on the shafts was removed by sonicating in a 50% solution of KOH dissolved in ETOH. The electrodes were then insulated with 2 to 4 coats of Epoxylite. The insulation at the tip was then removed during grinding of the facets and the latter were activated to form an iridium oxide surface. Most probes were approximately 1.5 mm in length. In one instance (2 x 2 array, IC-105), the lengths were 2.8 mm. The tips of the 7-electrode array were etched to a radius of curvature of 2-3 μm. This array was implanted stereotaxically in animal IC-100 and later salvaged for manual insertion in IC-105.

The photolithographic (University of Michigan) probes were composed of silicon with a silicone (MPX 4210) backing to provide a smooth surface to allow attachment to the vacuum holder on the electrode carrier. The probes were approximately 1.3 mm in length and had cross-sectional dimensions of 15 x 30 μm.

Surgical protocol. Craniectomies were made over the parietal cortex. The arrays were attached to a vacuum array holder which, in turn, was attached to an electrode carrier. The holder was centered over the crown of the gyrus suprasylvius. When the vacuum was released, the weighted cylindrical sleeve, positioned around the electrode holder, descends, implanting the array into the cortex (Fig. A). An attempt was made to avoid surface vessels. The dura, which had been cut into an L-shaped incision was then pulled over the electrode array and sutured.

Manually implanted probes were grasped with tweezers and then inserted through a 100 μm thick silicone template placed over the crown of the gyrus. This was to prevent the individual probes from sinking into the cortex after suturing the dura over the ball-shaped heads of the individual probes.

Autopsy and tissue processing. The durations of implant ranged from 2 to 69 days. At the end of these periods, the animals were sacrificed by transcardiac perfusion of Karnovsky's fixative followed by storage of the brain with electrodes in situ in the same type of fixative until autopsy the following day. Tissue samples were processed for paraffin embedment and serially sectioned either coronally or horizontally. The following stains were

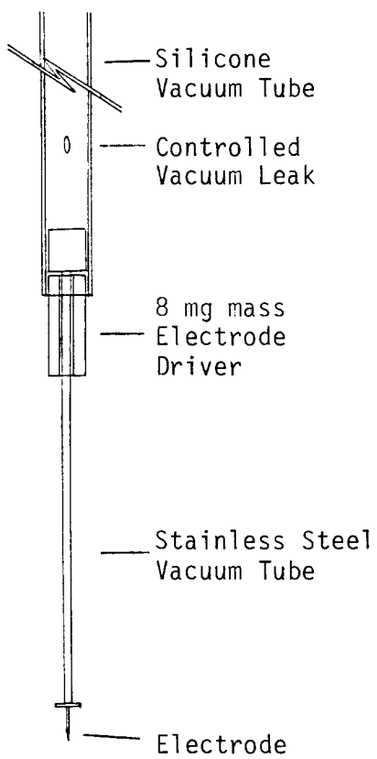

Fig. A. A microelectrode introducer attached to a stereotaxic carrier. The microelectrode is held in place by vacuum and positioned over the target area. Upon release of the vacuum a stainless steel sleeve weighing 8 mg is allowed to plunge the electrode into the brain

used: Nissl (for neurons), H & E (general stain) and Masson's Trichrome (for connective tissue).

HISTOLOGIC FINDINGS

Iridium Probe Sites.

Inflammation and infection. Acute inflammation (characterized by the presence of neutrophils) was never present except at some probe sites in IC-104 (48-hour implant duration, Fig. 1). Here, Type A adhesive presumably seeped through the silicone sheet where the electrodes had penetrated and traversed the length of the probe, acting as an irritant to the adjacent tissue. Lymphocytes were abundantly present at these same sites but these cells and neutrophils were less numerous in the contralateral hemisphere where Type A was not used. Aside from a cluster of lymphocytes and several neutrophils along one of 4 individual probes in the right hemisphere, the other iridium probe sites were accompanied by only occasional or a few lymphocytes, and the tracks were better defined (Fig. 2). We never found microorganisms or infection here or elsewhere in the entire series.

Microhemorrhages and cavitations: A wide spectrum of hemorrhagic responses was found, irrespective of whether or not the electrodes were inserted manually or with the use of the piston-driven device. For example, a complete absence of hemorrhage and cavitations was found at a 7-probe array site (IC-100, piston-driven insertion) (Fig. 3) while the same (salvaged) array inserted manually into IC-105 caused marked hemorrhage and subsequent cavitation (Fig. 4). Also, the manual insertion of 9 electrodes into IC-87 and IC-91 resulted in markedly different responses. The latter showed no hemorrhages or cavitations while the tracks in IC-87 were accompanied by several cavitations, the result of previous hemorrhages and subsequent scavenging of the extravasated RBC. In these 4 animals, the implantation time was 21 to 42 days. Several of the 4 probes left in IC-104 for only 48 hours were accompanied by extravasated RBC which had not yet been removed by phagocytes.

Glial scars. A relatively common finding at the sites of manually inserted single probe was a narrow glial scar, sometimes reaching as much as 400 μm in length, with one

Fig. 1. IC-104. Vertically cut paraffin section of the entry site of a passive epoxylite-coated iridium probe implanted in the gyrus suprasylvius for 2 days. The bevel angle was 20 degrees. All probe sites in this and succeeding micrographs were unstimulated. Numerous lymphocytes and neutrophils line the track (T). Type A adhesive was used to secure the tops of the probes and may have seeped through the silicone sheet and into the track sites. Presumably, the marked inflammatory response was incited by the adhesive. Nearby neurons appear essentially normal. A nearby blood vessel (V) is cuffed by lymphocytes. The loose cellular aggregate lining the track was easily disrupted during withdrawal of the probe at autopsy leaving ragged edges along the track. The 2-day implant period was insufficient for the formation of a connective tissue sheath. This and all succeeding micrographs are from paraffin sections taken through the track sites in the gyrus suprasylvius and stained with Nissl stain. Bar = 25 μm.

Fig. 2. Vertically sectioned iridium track in contralateral hemisphere of the same animal as shown in Fig. 1. Type A adhesive was not used at this site and the inflammatory reaction is minimal. The track (T) is clearly demarcated and extends far below the cortical neurons. At higher magnification, all tissue adjacent to the track appeared normal. Bar = 100 μm.


T
V
1

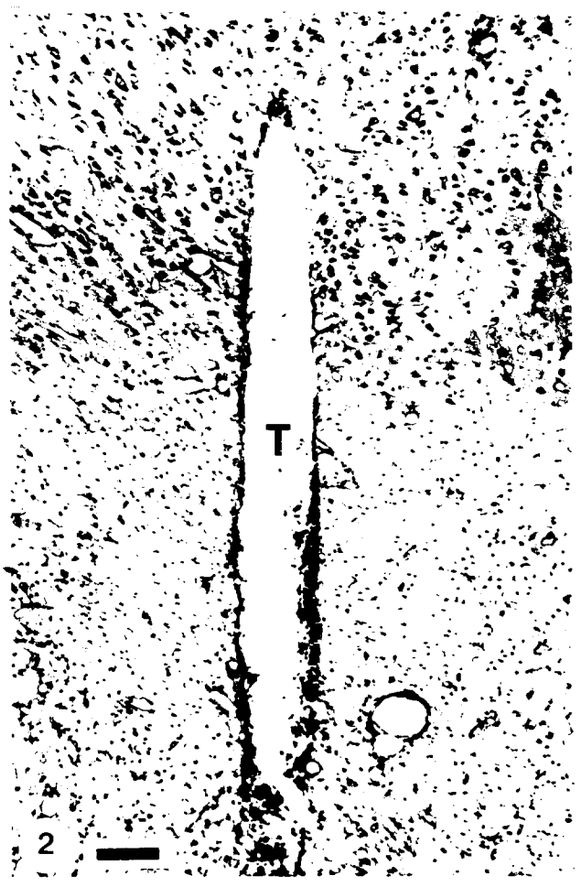
T
2

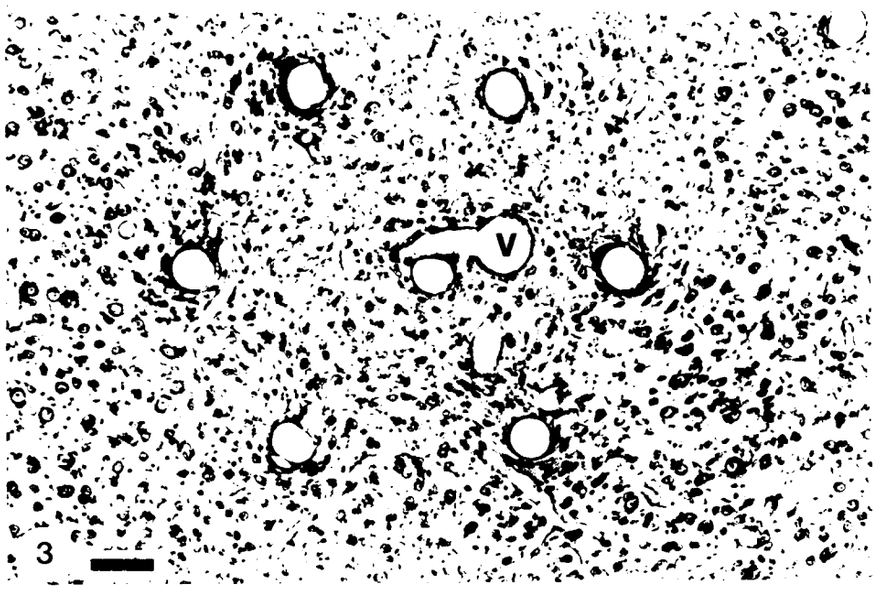

Fig. 3. IC-100. Horizontal sections through all tracks of a stereotaxically inserted 7-probe iridium array and left for 6 weeks. This section is approximately 320 μm deep and shows normal-appearing neurons among the tracks as well as a hypertrophied blood vessel (V). The latter was a common finding at sites of multiple probe arrays. Bar = 100 μm.

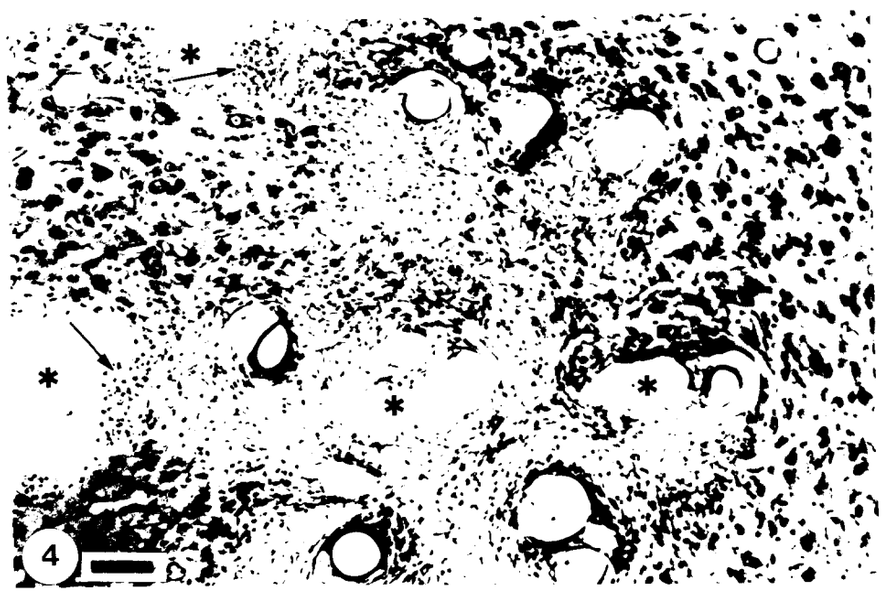

Fig. 4. IC-105. Cross-section through 7 tracks of the same array used in the previous micrograph. The array was inserted manually in this instance. Every track was in communication with a cavitation (asterisks) and these appear to be the sites of earlier hemorrhages. A few remaining clusters of macrophages (arrows) mark the sites of previous erythrophagocytosis. Bar = 100 μm.

end terminating at the tip of the track (Fig. 5). This was due to migration of the electrode. This scarring was diminished or absent at sites where multiple, fixed probes were inserted simultaneously. Another form of gliosis occurred at, and slightly below, the tips of some probes (Fig. 6). This took the form of clustered glial cells and strands of glia and connective tissue.

Neurons. Except in the path of glial scars, neurons were undamaged along the entire track and at the tip sites. A common finding was a somewhat "flattened" profile of neurons near the track. Presumably, this was due to mechanical forces exerted during penetration of the probes but the neurons did not appear hyperchromic or damaged.

Necrosis of neuropil adjacent to tracks. Tissue necrosis was not present at any site except occasionally where cavitations and rarefaction of tissue marked the site of a previous hemorrhage.

Vascular proliferation and hypertrophy. A few iridium probe sites were accompanied by vascular hyperplasia or hypertrophy. Among these were vascular hyperplasia along two of the 4 probe sites in IC-105 where numerous blood vessels closely skirted the tracks (Fig. 7). A similar finding was seen at one of the 8 tracks in IC-104. Moderate vascular hypertrophy was found between the 7 probes in IC-100 although vascular hyperplasia was not apparent at this array site. Compared to the track diameters in IC-87 (Figs. 8 & 9) the hypertrophied blood vessels between the tracks were large.

Photolithographic Probe Sites.

Inflammation and infection. Neither of these was present at any of the silicon probe sites.

Microhemorrhages and cavitations. These were not found at any site except adjacent to several probes at one of the two array sites in IC-99 (Fig. 10). Here, RBC were no longer present in the cavitations inasmuch as the duration of implant was 29 days and extravasated blood undoubtedly was scavenged by macrophages.

Glial scars. Gliosis was most prominent at or near the tips and ranged from slight to marked (Fig. 11). In some instances, the gliosis was confluent between adjacent probes while neighboring probes showed none (Fig. 12).

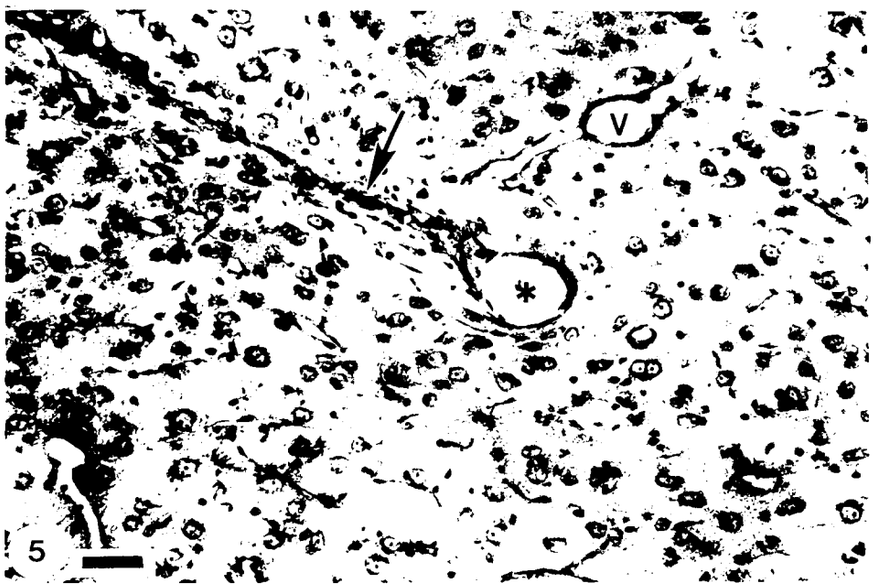

Fig. 5. IC-91. One of 9 tracks left by manually implanted individual iridium probes. Implant duration 3½ weeks. This section is at a depth of 400 μm and the track (T) is at the end of a 400 μm long glial scar (arrow) which was caused by earlier electrode movement. Nearby neurons appear normal. V = blood vessel. Bar = 50 μm.

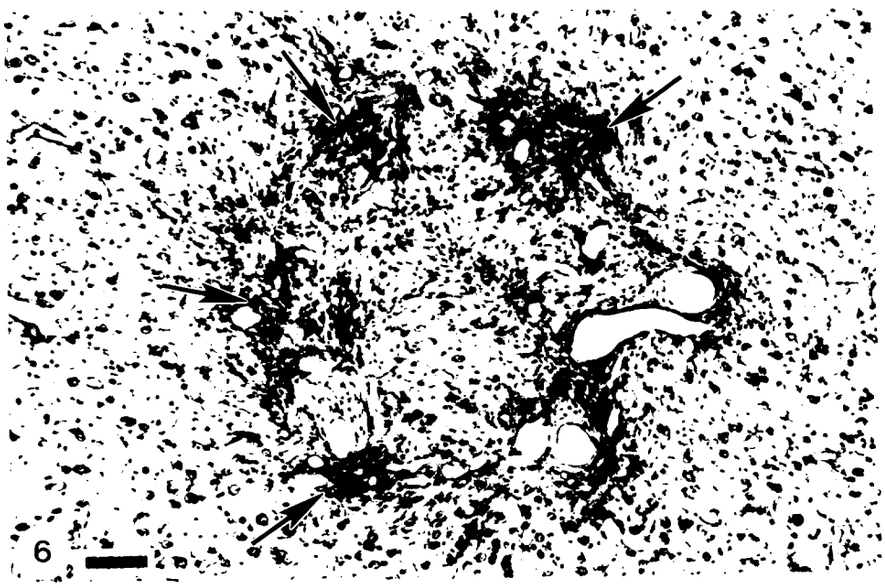

Fig. 6. IC-100. Section through or just below the tip areas of the 7-probe iridium array 7 weeks after implantation. The arrows indicate considerable gliosis at 4 tip sites. This section was taken slightly below the cortex and only a few isolated neurons are scattered throughout the micrograph. Bar = 100 μm.

Fig. 7. IC-105. An iridium probe site 5 weeks after implantation. This vertical section has captured an oblique segment of the track which, here, is 1,450 μm below the pia and extends below the cortical neurons. The vertical "scars" above and below the track represent the oblique, grazing cut through the CT sheath. Note the marked vascular hyperplasia skirting the CT sheath from the molecular layer (top edge of micrograph) to the lowermost extent of this segment of the track. Bar = 100 μm.

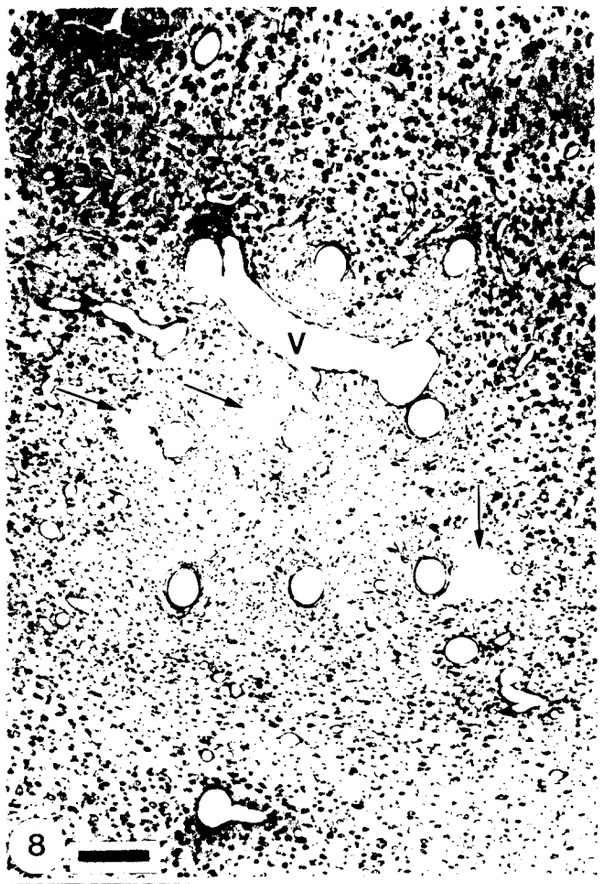

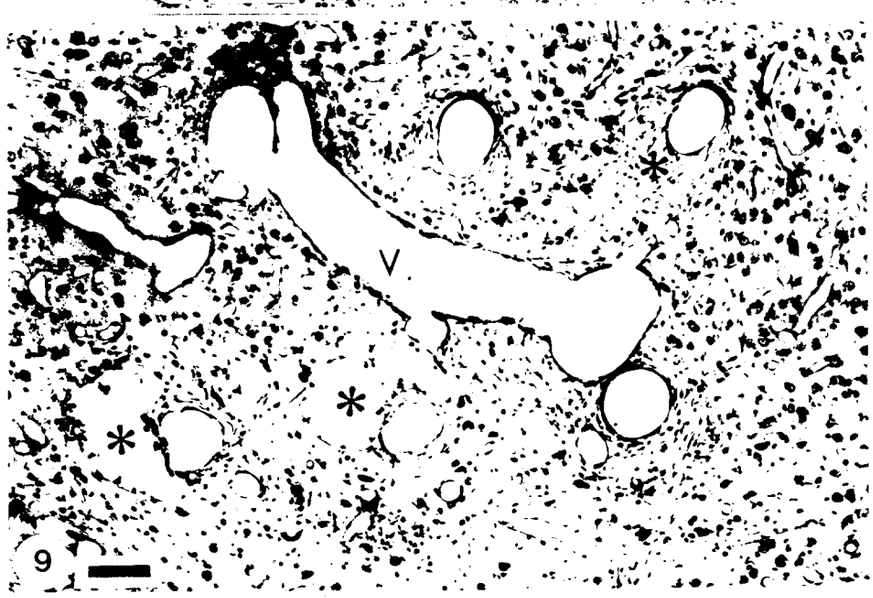

Figs. 8 & 9. IC-87. Low and high magnifications, respectively, of the 9-probe iridium array site three weeks after implantation. Fig. 8 shows all tracks in transverse section at a level 800 μm below the pia. Several tracks are associated with cavitations (arrows), which represent sites of earlier hemorrhages. V = hypertrophied blood vessel. Fig. 9 shows, at higher magnification, the nature of the cavitations (asterisks). These have ragged edges which are incompletely lined by macrophages and lack a limiting membrane. The enlarged blood vessel (asterisk) appears in continuity with two tracks. Bars = 200 and 100 μm, respectively.

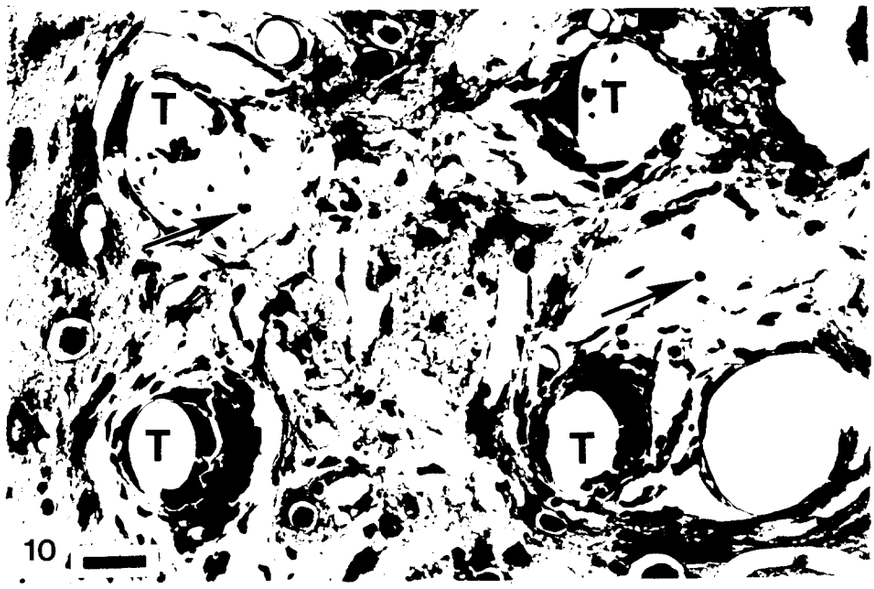

Fig. 10. IC-99. Transverse section through the tracks (T) of 4 of 16 photolithographic probes 400 μm below the pia. Implant duration 4 weeks. Every track is associated with a cavitation and some of these contain lingering macrophages (arrows). There is rarefaction and a paucity of neurons between the tracks. Bar = 25 μm.

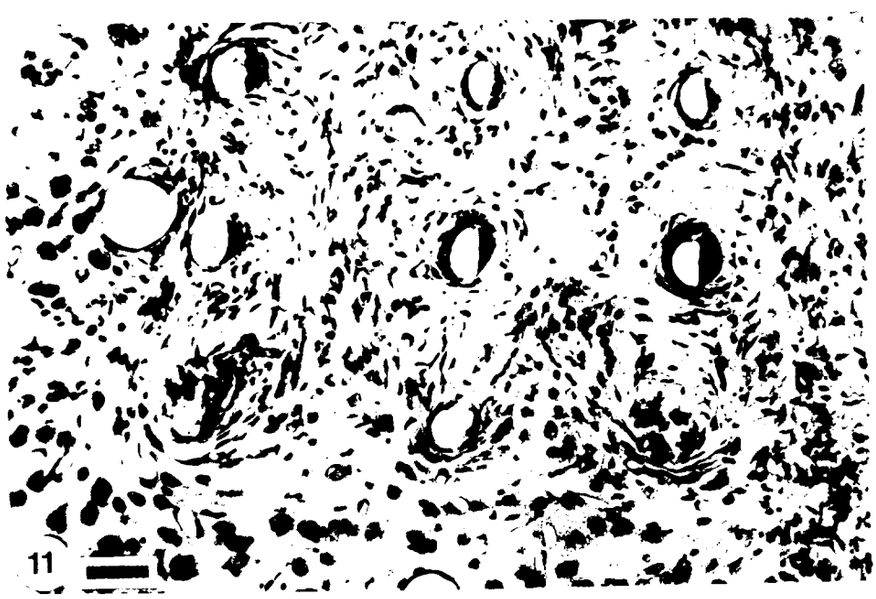

Fig. 11. IC-99. Transverse section through 9 of 6 University of Michigan photolithographic probe sites 4 weeks after implantation. The marked gliosis has eradicated the normal architecture of all intervening tissue, including virtually all neurons. Bar = 50 μm.

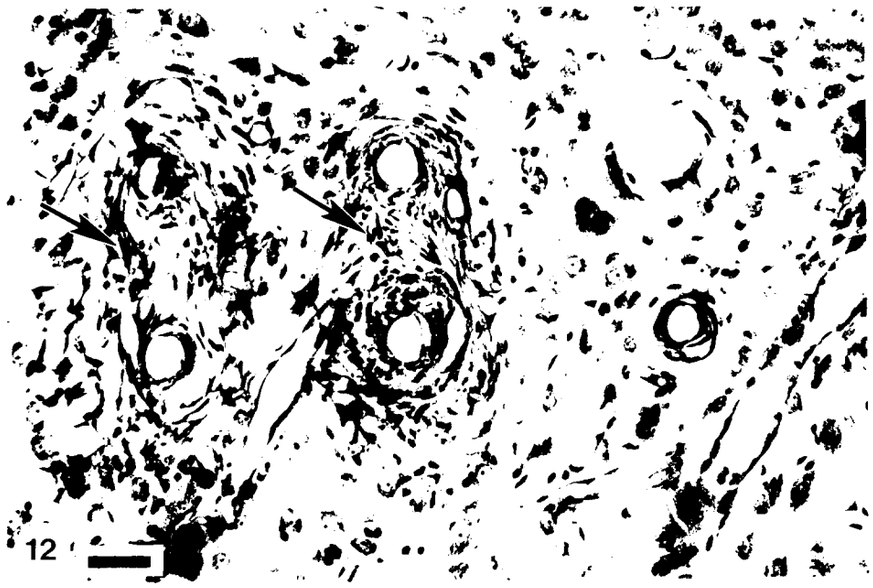

Fig. 12. IC-98. Six of 16 tracks 3½ weeks after implantation of a University of Michigan photolithographic array. Note the gliosis (arrows) around 4 tracks while sparing 2 tracks (right side of micrograph). The gliosis has compromised the number of neurons in this area although other, nearby neurons appear normal. Bar = 50 μm.

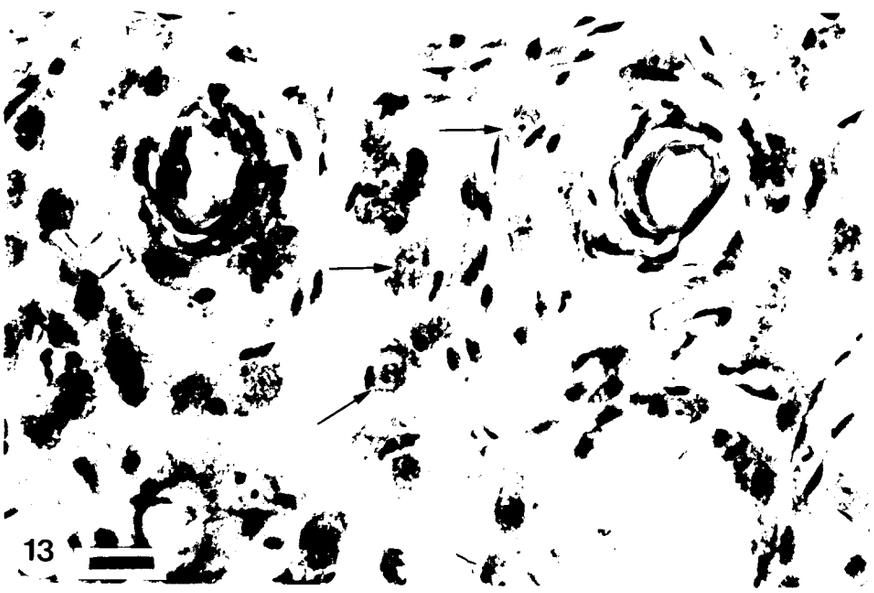

Fig. 13. Same array site as shown in Fig. 12 but 200 μm lower. Gliosis is not present at this level and there is no hemorrhage or cavitation. The neurons (arrows) appear normal. There appears to be avulsion of the sheath around one track (lower right of micrograph). Bar = 25 μm.

Neurons. Neurons adjacent to the tracks appeared normal (Figs. 13 & 14) except in a few instances where gliosis between the tracks was marked (Fig. 11).

Necrosis of neuropil adjacent to tracks. Necrosis, per se, was not found. At sites where extensive gliosis was present, loss of neurons and adjacent tissue (between electrodes) was replaced by gliotic scarring.

Vascular proliferation and hyperplasia. These were uncommon at most array sites but in a few instances (Fig. 15) both phenomena were present concurrently and were found primarily between the tracks. Some of the larger blood vessels measured as much as 90 μm in diameter.

Probe misalignment. The transversely sectioned 4 x 4 tracks at two photolithographic array site showed two types of probe misalignment. One type was a mediolateral misalignment of some of the probes so that their tracks were within 40 μm of contacting their nearest neighbor (Fig. 16). The second type of probe misalignment was an approximately 70 μm anterior-posterior permanently fixed shift of one of the 4 rows of probes. The "shift" was visible high in the array (i.e., in the superficially located molecular layer) (Fig. 17).

The second type of misalignment probably occurred during assembly of the array. In support of this is the 70 μm misalignment near the "hilt" of four in-line probes as evidenced in Fig. 17, where the misalignment was present high in the tracks left in the molecular layer. At this proximity to the matrix, the rigidity of the proximal part of each probe would be relatively great and would probably preclude deviation of the probe, especially in the anterior-posterior (greater) dimension of 15 x 30 μm cross-section of the probes.

DISCUSSION

The etiology (ies) of microhemorrhages adjacent to the probes is unclear. In many instances, the beveled tips on the iridium probes may be the most responsible factor, acting to sever the blood vessels. On the other hand, the rate of penetration must be investigated further, inasmuch as a beveled electrode tip might still gently nudge aside a blood vessel

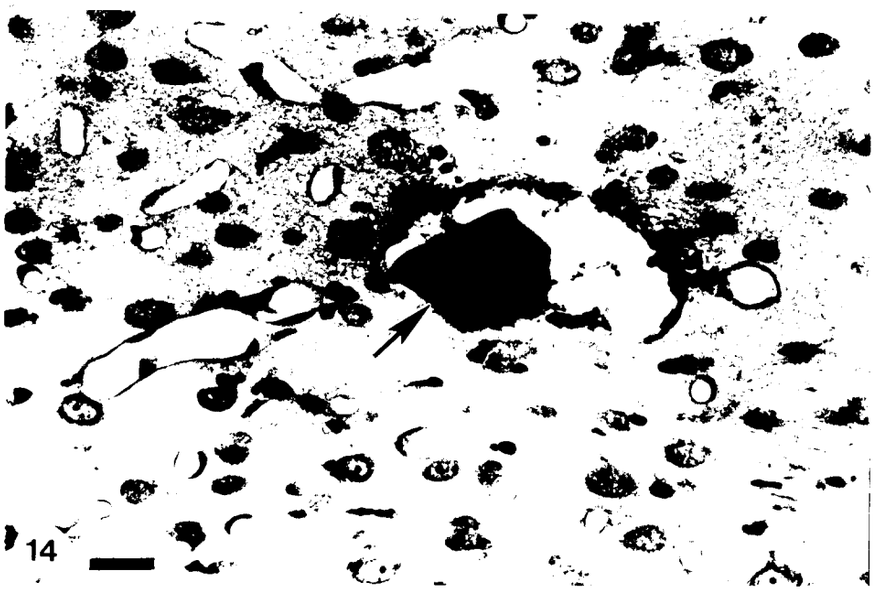

Fig. 14. IC-105. Site of the single University of Michigan photolithographic probe 5 weeks after implantation. The silicon probe was not visible at autopsy, consequently, the track site was cross-sectioned with the probe in situ (arrow). There is some mechanical disruption of the track although the adjacent tissue, including all neurons, appears normal. Bar = 25 μm.

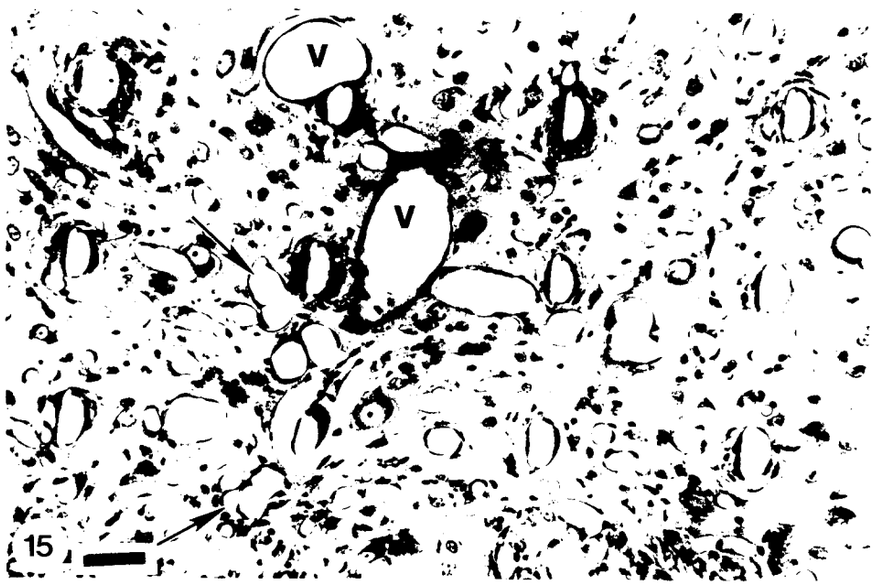

Fig. 15. IC-94. Transverse section through 12 of 16 University of Michigan photolithographic probe sites 10 weeks after implantation. Both vascular hyperplasia (arrows) and vascular hypertrophy (V) are present near the probe sites. All other tissue, including neurons, appears normal. Bar = 50 μm.

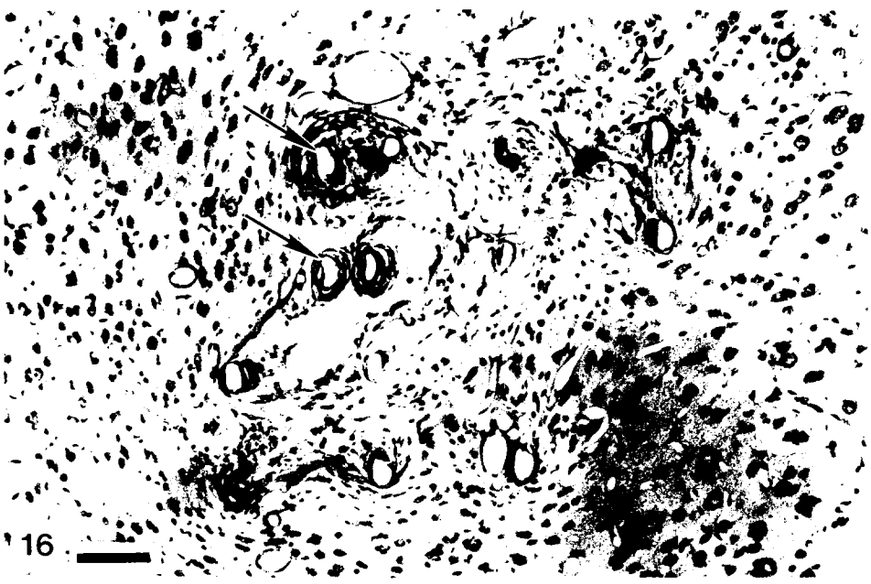

Fig. 16. IC-93. Transverse section through the lowermost portions of the 4 x 4 photolithographic array site. Implant duration 8 weeks. The section has passed below 3 of the 16 tips. Note the deviation of 2 probes (arrows) so that they have become encapsulated and rest near the probes in the adjacent row. Cavitations are associated with several tracks int he left part of the micrograph. Bar = 100 μm.

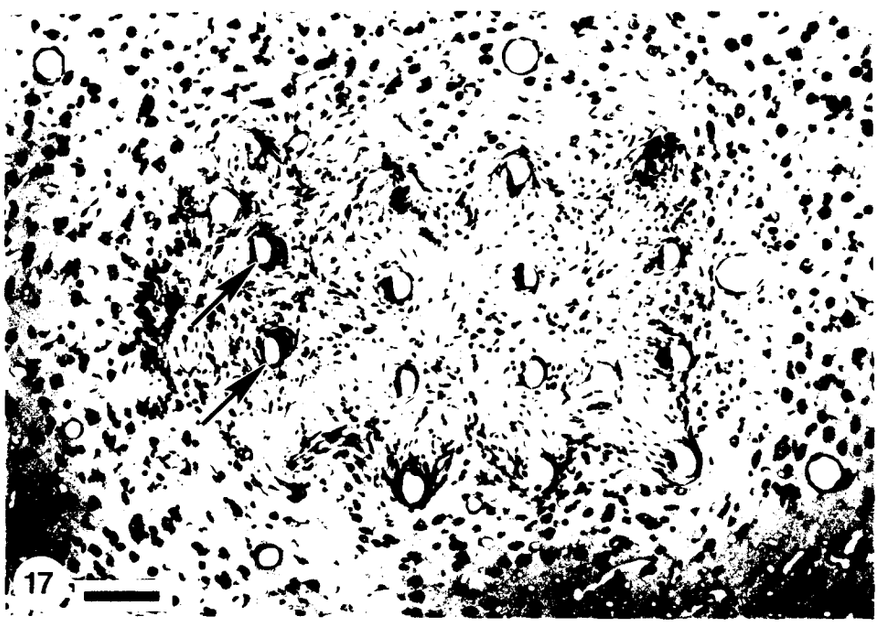

Fig. 17. IC-99. Implant duration 7 weeks. Sixteen silicon probe sites are present in cross section. The section passes through the molecular layer, hence, the absence of neurons between the tracks and around a portion of the array site. The arrows indicate an anterior-posterior misalignment of the probes in the left-hand row. Bar = 100 μm.

when penetration is slow. The preliminary attempt to use a non-beveled probe (the 7-probe array in IC-100 and IC-105) shows the wide variability in responses. In the first instance, there was no bleeding whereas animal IC-105 sustained considerable bleeding at the probe sites, culminating in cavitation after the RBC were scavenged by macrophages.

There has been considerable variation of the extent of damage seen at various depths along the tracks. We would like to emphasize the importance of evaluating the electrode sites at all levels from the pia to the tips of the electrodes, as demonstrated in this report and others (Campbell et al, 1989). Even large arrays of electrodes inflict very little damage at one depth as opposed to appreciable damage at a different depth.

Glial scars are one of the most common sequelae of CNS trauma, including penetration of microprobes. The fact that some tracks show no such responses while neighboring tracks show considerable gliosis (Fig. 12) might indicate that some surface contaminant has elicited such a response. Another cause for this reaction could be movement of the probe with greatest excursion at the tip, especially if the dura had been exerting mechanical force on the superstructure of the probe, thus causing a "rocking" or "pendulum" type of motion of the entire shaft of the probe. Methods of increasing the stability of individual or multiple electrodes must be investigated and perfected. This includes methods of securing the dura after implantation of the probes as well as optimal routing of cables in active arrays.

With regard to necrosis of tissue adjacent to the tracks, the speed of penetration appears not to be a factor other than the indirect damage following rupture or cutting of blood vessels and subsequent hemorrhage into the parenchyma.

It is to be expected that, following the trauma of electrode penetration, there would be a need for increased local blood flow to aid in tissue reconstructive, and presumably, this accounts for the vascular hyperplasia and hypertrophy reported here.

Presumably, misalignment of 3-dimensional silicon probes was due to two factors. In the one instance, the thin (15 μm) dimension of the probes allows for considerable flexion during insertion. This could lead to a mediolateral "skewing" of individual probes. It is unlikely that an entire row of 4 probes was misaligned during assembly inasmuch as only 2 of 4 probes had come to final rest adjacent to their neighbors (see Fig. 16).

A second source of electrode misalignment results during electrode fabrication when the 4 "combs," each having multiple in-line electrodes, are not accurately affixed to the matrix. The result is an offset in which the electrodes are in alignment in one direction but not when viewed at 90° to the first direction.

Thirdly, when the electrodes are affixed to the matrix at an angle, other than truly vertically, the inevitable results will be a simultaneous slashing of the cote by all such electrodes. It is to be expected that numerous blood vessels would be ruptured by such action. Due to the deleterious effects (bent tips, possible contaminating material) of reimplanting salvaged electrode arrays, we have decided to use only pristine arrays in both acute and chronic experiments.

Clearly, considerable study must be devoted to the many important factors leading to successful microprobe implants. Among these are: tip configuration of the probes, speed of insertion, ideal configuration and routing of cables for ultimate use in active implants. The latter is critical to prevent tension on implanted arrays. Further, the proper methods of incising and reapproximating the dura at the operative site will be crucial to success. Finally, the use of ideal adhesives for stabilizing the implants must be studied further.

REFERENCES

Campbell, P.K., Normann, R.A. and Horch, K.W. A chronic intracortical electrode array: Preliminary results. J. Biomat. Res. : Applied Biomat., 23:245-259, 1989.

WORK NEXT QUARTER

We will continue our evaluation of mechanical injury that results during implantation of penetrating microelectrodes of varying tip configurations. We will also compare manual and stereotaxic insertion techniques and speed of insertion using both epoxy-coated iridium and silicon (photolithographic) electrodes.